Title

Cell wall ester modifications and volatile emission signatures of plant response to abiotic stress

Journal

Plant Cell & Environment, 45(12)

ISSN

0140-7791

Authors

Jardine, Kolby J

Dewhirst, Rebecca A

Som, Suman

et al.

Publication Date

2022-12-01

DOI

10.1111/pce.14464

Cell wall ester modifications and volatile emission signatures of plant response to abiotic stress

Kolby J Jardine[1], Rebecca A Dewhirst[1], Suman Som[1], Joseph Lei[1], Eliana Tucker[1], Robert P Young[2], Miguel Portillo-Estrada[3], Yu Gao[4], Luping Su[5], Silvano Fares[6,7], Cristina Castanha[1], Henrik V. Scheller[4,8], Jenny C Mortimer[4,9]*

[1] Climate and Ecosystem Science Division, Lawrence Berkeley National Lab, Berkeley, CA 94720, USA (kjjardine@lbl.gov)

[2] Environmental Molecular Sciences Laboratory, Pacific Northwest National Lab, Richland, WA, USA

[3] Research group PLECO (Plants and Ecosystems), Department of Biology, University of Antwerp, Wilrijk, Belgium

[4] Joint BioEnergy Institute, Lawrence Berkeley National Lab, Emeryville, CA USA

[5] Tofwerk USA, Boulder, CO, USA

[6] Institute of BioEconomy, National Research Council, Rome, Italy

[7] Department of Environmental Science, Policy, and Management, University of California at Berkeley, CA USA

[8] Department of Plant and Microbial Biology, University of California at Berkeley, CA USA

[9] School of Agriculture, Food, and Wine, University of Adelaide, Glen Osmond, SA, Australia

Highlight: Acetic acid/methanol leaf emissions ratios are a sensitive indicator of the balance between plant growth and defense during drought.

Abstract

Growth suppression and defense signaling are simultaneous strategies that plants invoke to respond to abiotic stress. Here, we show that the drought stress response of poplar trees (*Populus trichocarpa*) is initiated by a suppression in cell wall derived methanol (MeOH) emissions and activation of acetic acid (AA) fermentation defenses. Temperature sensitive emissions dominated by MeOH (AA/MeOH < 30%) were observed from physiologically active leaves, branches, detached stems, leaf cell wall isolations, and whole ecosystems. In contrast, drought treatment resulted in a suppression of MeOH emissions and strong enhancement in AA emissions together with volatiles acetaldehyde, ethanol, and acetone. These drought-induced changes coincided with a reduction in stomatal conductance, photosynthesis, transpiration, and leaf water potential. The strong enhancement in AA/MeOH emission ratios during drought (400-3,500%) was associated with an increase in acetate content of whole leaf cell walls, which became significantly $^{13}C_2$-labeled following the delivery of $^{13}C_2$-acetate via the transpiration stream. The results are consistent with both enzymatic and non-enzymatic MeOH and AA production at high temperature in hydrated tissues associated with accelerated primary cell wall growth processes, which are downregulated during drought. While the metabolic source(s) require further investigation, the observations are consistent with drought-induced activation of aerobic fermentation driving high rates of foliar AA emissions and enhancements in leaf cell wall *O*-acetylation. We suggest that atmospheric AA/MeOH emission ratios could be useful as a highly sensitive signal in studies investigating environmental and biological factors influencing growth-defense trade-offs in plants and ecosystems.

Keywords and Abbreviations:

Acetic acid (AA), aerobic fermentation, methanol (MeOH), AA/MeOH ratio, cell wall esters, pectin, xylan, plant drought stress, growth suppression, volatile organic compounds (VOCs)

Introduction

Fast growing trees are increasingly utilized as a sustainable source of bioproducts and biofuels as well as carbon farming, urban greening, hillslope stabilization, and marginal land restoration and re-forestation (Ragauskas *et al.*, 2006; Furtado *et al.*, 2014). Field observations have consistently shown that non-water limited poplar plantations have high growth and productivity rates, but are highly sensitive to drought (Ji et al., 2020). For example, poplar trees in northern China have experienced large-scale dieback and mortality in recent years (Ji et al., 2020). An estimated 79.5% of the area of the poplar forests have experienced severe degradation with an observed trend of narrower tree-ring widths of intact trees together with reduced soil moisture. These observations highlight the need to understand the mechanisms of poplar forest growth suppression and die-back in response to drought stress (Ji et al., 2020). Prolonged excessive water loss via transpiration not replaced by water uptake from the soil can result in drought-induced tissue senescence and mortality, thereby converting individual plants and ecosystems from net sinks of CO_2 to net sources (McDowell et al., 2008; Jardine et al., 2015; Liu et al., 2021). Understanding the biological mechanisms and environmental thresholds that determine plant responses to drought stress is critical for predicting how the structure and function of managed ecosystems will respond to environmental change (McDowell *et al.*, 2008; Dewhirst et al., 2021a).

Previous studies have characterized the sequence of plant hydraulic, physiological, biochemical, and structural changes associated with reversible and irreversible responses to drought stress. For example, leaf dehydration responses of ten angiosperm species showed stomatal closure and a decrease in xylem conductance occurring first as a reversible response (Trueba *et al.*, 2019). This

3

was followed by reaching the turgor loss point, xylem embolism, and the cessation of transpiration as a critical irreversible threshold following which further irreversible damage occurred including to the membranes, pigments, and other components of the photochemical system in the chloroplast (Trueba *et al.*, 2019). While ecosystem response to water deficit can be detected by current remote sensing methods such as solar induced fluorescence (SIF) (Sun *et al.*, 2015), and various normalized vegetation indices such as the Normalized Difference Vegetation Index (NDVI) (Peters *et al.*, 2002) and Enhanced Vegetation Index (EVI) (Aulia *et al.*, 2016), these generally only identify extreme drought and the associated irreversible loss of major leaf function such as transpiration and net carbon assimilation. For example, in 2-yr old *Populus deltoides* individuals, while strong responses of net photosynthesis and stomatal conductance to initial water stress were observed at the leaf level, SIF showed relatively minimal changes (Helm *et al.*, 2020). It was concluded that the value of SIF as an accurate estimator of net photosynthesis may decrease during mild stress events of short duration, especially when the response is primarily stomatal and not fully coupled with the degradation of photosynthetic capacity. This highlights the need for new methods to better understand the biochemical, physiological, and ecological mechanisms *in situ* associated with the onset of drought stress including processes that alter plant growth and defense balances and their associated changes in leaf CO_2 and H_2O gas exchange fluxes.

A common thread among many of the biochemical and physiological processes that determine ecosystem dynamic responses to climate change variables are alterations in plant cell wall chemical composition, structure, and function (Dewhirst et al., 2020a,b). A large proportion of the plant cell wall polymers can be heavily modified with methyl and *O*-acetyl ester groups

4

which may play important roles in cell growth and tissue development (Peaucelle et al., 2012), proper xylem (Yuan et al., 2016) and stomatal functioning (Amsbury et al., 2016), central carbon and energy metabolism (Jardine et al., 2017), and stress communication and signaling (Novaković et al., 2018). For example, wood of hybrid poplar trees, one of the fastest growing temperate trees in the world, is composed of lignin (22%), cellulose (40%), hemicellulose (20%) dominated by the *O*-acetylated polysaccharide glucuronoxylan, and other polysaccharides such as pectins (18%), which can be both heavily *O*-acetylated and methyl-esterified (Sannigrahi et al., 2010). The two main components of the plant primary cell wall, the pectin matrix and the cellulose/xyloglucan network, are constantly remodeled to support dynamic morphological and physiological processes from daily growth and stress response patterns, to developmental changes over longer time scales (Chebli and Geitmann, 2017). This remodeling is regulated, in part, by a number of loosening and stiffening agents including pectin and xylan methyl and acetyl esterases which catalyze the hydrolysis of cell wall esters on the wall. The hydrolysis of methyl and *O*-acetyl esters leads to rapid physicochemical changes in the cell wall and the release of methanol (Fall, 2003) and acetic acid (Scheller, 2017). Given that cell wall methyl and *O*-acetyl esters are known to modify cell wall elasticity/rigidity (Peaucelle et al., 2011), and previous observations have shown links between bulk cell wall elasticity and water relations (Roig-Oliver et al., 2020), they may play important roles in the response to drought (Ganie and Ahammed, 2021). However, how the degree of cell wall esterification varies with abiotic stress is largely unknown (Pauly and Keegstra, 2010; Gille and Pauly, 2012).

The source of cell wall *O*-acetyl esters is thought to be primarily acetyl-CoA. Acetyl-CoA is a central component of plant carbon and energy metabolism, generated independently in many

5

organelles such as through the reaction catalyzed by pyruvate dehydrogenase (PDH) during aerobic respiration (mitochondria) and fatty acid biosynthesis (chloroplasts). First described as the 'PDH bypass pathway' in yeast, acetyl-CoA production in plants under aerobic conditions has also been linked to enzymes involved in fermentation like pyruvate decarboxylase and acetaldehyde dehydrogenase (Wei et al., 2009). Recently, acetate accumulation produced by aerobic fermentation during drought stress was shown to coordinate plant response to drought stress through a global reprogramming of transcription, cellular metabolism, hormone defense signaling, and chromatin modification mediated by protein acetylation (Kim et al., 2017).

In this study, we first hypothesize that during rapid growth under well-watered conditions, methanol (MeOH) and acetic acid (AA) from leaf cell wall ester hydrolysis is the main source of foliar MeOH and AA emission to the atmosphere during well-watered conditions. Moreover, ester hydrolysis reactions increase as a function of temperature through both enzymatic and non-enzymatic ester hydrolysis reactions. Second, we hypothesize that due to hydraulic limitations to growth during drought stress, cell wall-derived MeOH production is inhibited. Together with reductions in stomatal conductance, we predict that drought-induced suppression of growth rates will also suppress leaf MeOH emissions. In contrast to well-watered conditions where cell wall esters are the dominant source of MeOH and AA emissions, we hypothesize that aerobic fermentation becomes the dominant source of leaf AA emissions during drought stress. Finally, in addition to acetate-mediated signaling mechanisms associated with protein acetylation (Kim et al., 2017), we hypothesize that additional biopolymers such as cell wall polysaccharides, may also respond with increased acetylation during drought responses.

6

We aimed to test these hypotheses by quantifying drought induced changes in bulk leaf cell wall composition as well as *O*-acetylation content in 2-year old potted California poplar (*Populus trichocarpa*) trees. Delivery of 10 mM $^{13}C_2$-acetate solutions to canopy leaves via the transpiration stream were used to evaluate the metabolic connection between leaf free acetate and *O*-acetylation of bulk leaf cell wall polysaccharides. During experimental drought stress, we collected real-time patterns in MeOH and AA emissions together with the fermentation volatiles acetaldehyde, ethanol, and acetone in parallel with leaf gas exchange (net photosynthesis, transpiration, stomatal conductance) and leaf water potential measurements. Complementary environmental sensitivities of MeOH and AA gas exchange studies are presented on hydrated leaf bulk cell wall preparations and physiologically active leaves, branches, and whole ecosystems. We define the AA/MeOH emission ratio as a potentially sensitive atmospheric indicator of environmental and biological conditions that favor rapid plant growth versus suppressed growth and defense activation.

Materials and Methods

Leaf physiological impacts during an experimental drought

Thirty California poplar (*Populus trichocarpa*) saplings were obtained from a commercial supplier (Plants of the Wild, USA). The trees were transferred into #2 pots (6.59 L) with Supersoil planting media (Scotts Co., USA) and maintained for two years in the UC Berkeley Oxford Tract greenhouse under natural lighting supplemented with LED lighting (6:00–20:00 light period; Lumigrow 325 Pro, USA). The thirty potted trees reached a stem diameter (5 cm) and height (1.5 m) just prior to the commencement of experimental measurements. A subsection (15 individuals) of the 2-year old trees had water withheld for one week (drought plants), while a

7

control group (15 individuals) continued to receive morning, afternoon and night water supply. For each individual throughout the controlled drought experiment, one mature leaf was selected for leaf gas exchange measurements in the greenhouse using a portable Li6800 photosynthesis system including stomatal conductance (g_s, mol m^{-2} s^{-1}), net photosynthesis (A, μmol m^{-2} s^{-1}), and transpiration (E, mmol m^{-2} s^{-1}) under standard environmental conditions (400 ppm reference CO_2, 25 mmol mol^{-1} reference absolute humidity, 1000 μmol m^{-2} s^{-1} photosynthetically active radiation, 600 μmol s^{-1} leaf chamber air flow rate, 31 °C heat exchange block). Immediately following leaf gas exchange measurements in the morning, leaf water potential was determined using a nitrogen pressure chamber instrument (Model 600, PMS Inst., USA). The leaf was detached from the tree using a razor blade, and the petiole sealed in the leaf pressure chamber where nitrogen pressure slowly increased until liquid water was visible from the petiole. Following the gas exchange and leaf water potential measurements, a second mature leaf was taken from each of the 30 trees and frozen on dry ice and stored at -80°C prior to cell wall analysis. Leaf gas exchange and water potential measurements and frozen leaf samples were collected from one mature leaf for each of the 15 control and 15 drought-treated individuals at time = 0, 1, 4, and 7 days.

Leaf Alcohol Insoluble Residue (AIR) preparations

Cell wall preparations (alcohol insoluble residue; AIR), were extracted from poplar leaf samples collected during the drought and $^{13}C_2$-acetate labeling experiments. Leaves were flash frozen in liquid nitrogen and then ground to a powder with a pestle and mortar on dry ice. The ground samples were incubated in 96% (v/v) ethanol at 70°C for 30 minutes. The supernatant was discarded and the samples washed successively in 100% ethanol, 2:3 chloroform: methanol

8

(twice, with shaking for at least 1 hour), 60% ethanol, 80% ethanol and 100% ethanol. Samples were centrifuged and the supernatant discarded between each washing step. The resulting AIR was dried in a speedvac and destarched for the monosaccharide analyses using amylase, amyloglucosidase and pullulanase (Megazyme Ltd., Ireland) as previously described (Sechet *et al.*, 2018).

Bulk *O*-acetyl ester content of AIR samples was carried out using a commercial kit (Acetate Assay Kit, BioVision, CA, USA). AIR samples (2.5 mg) were saponified with NaOH (1 M, 125 µL) for 16 hours then neutralized with 1 M HCl. The samples were centrifuged (10 minutes at 15000 rpm) and 5 µL of the supernatant was transferred to a 96-well plate. The samples were treated with the assay kit enzymes and plates incubated at room temperature for 40 mins. Absorbances were measured at 450 nm on a 96-well plate reader (SpectraMax M2; Molecular Devices, CA, USA). Total *O*-acetyl content of the AIR samples (µg/mg AIR) were determined by including a six-point calibration on each plate using the included standard.

In order to determine bulk leaf cell wall monosaccharide composition, destarched AIR (200 µg) was incubated in 2M trifluoroacetic acid (400 µl) at 120°C for 3 hours. The supernatant was collected after centrifugation. The pellet was washed with 200 µl milliQ water, centrifuged and the supernatant collected. The combined supernatants from each sample were dried in a speedvac. The sample was resuspended in 200 µl milliQ water, filtered on a 0.22 µm centrifuge filtration plate then analyzed for monosaccharide composition using high-pressure anion-exchange chromatography (Dionex-ICS 5000, Thermo Fisher Scientfic, CA, USA).

9

Real-time AA and MeOH emission measurements

Experimental details of the leaf, branch, and ecosystem gas exchange methods to determine AA and MeOH emissions, as well as the detached stem, detached leaf, and hydrated AIR temperature response curves can be found in the supplementary methods. Briefly, emission rates of MeOH and AA were quantified in real-time (roughly 2.5 measurements per minute) using a high sensitivity quadrupole proton transfer reaction mass spectrometer (PTR-MS, Ionicon, Innsbruck Austria, with a QMZ 422 quadrupole, Balzers, Switzerland). The PTR-MS was regularly calibrated to a primary standard by dynamic dilution (Supplementary **Figure S1**). AA and MeOH emissions were determined using PTR-MS at the leaf level using an environmentally controlled leaf photosynthesis system (Model 6800, Licor Biosciences, USA), branch level using a custom 5.0 L transparent Tedlar gas exchange enclosure with artificial lighting, and from a temperature-controlled chamber used for detached leaf, stem, and hydrated AIR AA and MeOH emission studies (Model 150 Dynacalibrator, +/- 0.01 C temperature accuracy, Vici Metronics, USA). Together with air temperature, continuous above canopy ambient AA and MeOH concentrations during the growing season were made at a poplar plantation in Belgium (Portillo-Estrada *et al.*, 2018), a mixed hardwood forest in Alabama (Su *et al.*, 2016), and above a citrus grove in California (Park *et al.*, 2013). Vertical ecosystem fluxes of MeOH and AA were estimated at the Belgium field site using the technique of eddy covariance employing high frequency vertical wind and MeOH and AA concentration measurements (Portillo-Estrada *et al.*, 2018). While ecosystem concentration and flux measurements MeOH were collected at all three sites using eddy covariance with PTR-TOF-MS, only the Belgium poplar plantation reported ecosystem scale AA flux data. At the Alabama mixed forest site, AA fluxes were not reported

10

232 (Su *et al.*, 2016) and at the citrus grove in California, AA fluxes were reported to suffer from
233 gaseous AA surface interactions within tubing (Park *et al.*, 2013). Therefore, at the Alabama and
234 California sites, diurnal ambient concentrations of MeOH and AA were analyzed instead of
235 fluxes as a function of air temperature.
236
237 ***Long-distance $^{13}C_2$-acetate transport in the transpiration stream and leaf cell wall O-***
238 ***acetylation interactions***
239 In order to evaluate the possibility of long-distance metabolic interactions between plant tissues
240 mediated by acetate in the transpiration stream, including influencing *O*-acetylation dynamics of
241 cell walls, $^{13}C_2$-acetate labeling studies were carried out on individual *P. trichocarpa* trees
242 transferred from the greenhouse to the laboratory. $^{13}C_2$-acetate delivery to leaves was
243 accomplished using detached branches (N = 3 branches, 1 branch/individual) placed in a 10 mM
244 solution of sodium $^{13}C_2$-acetate (Sigma-Aldrich, USA) for 2 days inside an environmentally
245 controlled growth chamber (Percival Intellus Control System, USA) maintained at 27.5 °C
246 daytime temperature (6:00–20:00; 30% light) and 23 °C nighttime temperature (20:00-6:00).
247 After 2 days, the branches took up roughly 30-40 ml of the $^{13}C_2$-acetate solution. In addition, a
248 single individual of 2.1 m height was placed in the laboratory under automated daytime lighting
249 with continuous daytime (150 µl min^{-1}) and nighttime (70 µl min^{-1}) xylem injection at the base of
250 the stem with a 10 mM sodium $^{13}C_2$-acetate solution (1,176 ml injected over 7 days using a flow
251 controlled M6 Pump, Valco Instruments Co. Inc., USA). Following the $^{13}C_2$-acetate labeling
252 period (branch: 2-day, tree: 7-day), a mature leaf was removed and flash frozen under liquid
253 nitrogen and stored at -80 °C before isolating whole leaf cell walls through the generation of

11

AIR. Leaf AIR samples were also prepared from detached branches fed with water and 10 mM acetate with natural $^{13}C/^{12}C$ abundance as controls. Experimental details of the AIR saponification followed by ^{13}C-labeling analysis of the released acetate can be found in the supplementary methods.

Results

Leaf gas exchange and water potential responses to experimental drought

Following the cessation of soil moisture additions on Day 0, large impacts on leaf water use and CO_2 metabolism could already be observed by Day 1 of the drought (**Figure 1**). For example, mean stomatal conductance (g_s) values of drought treated plants declined from 1.1 mol m^{-2} s^{-1} on day 0 to 0.026 mol m^{-2} s^{-1}, representing a 97% decrease. These low conductance values were maintained throughout the drought treatment on day 4 and 7. As expected from a strong drought-induced decrease in g_s, leaf gas exchange of CO_2 and H_2O in the light showed a large suppression in drought-treated plants. Under standard environmental conditions, average net photosynthesis (A) decreased from 13.4 μmol m^{-2} s^{-1} on Day 0 to -0.5 μmol m^{-2} s^{-1} on Day 1, representing a 104% decrease and loss of net carbon assimilation. These near zero and often negative net CO_2 assimilation values continued in the drought plants through days 4 and 7. Likewise, leaf transpiration (E) decreased by 94% on Day 1 as a result of the experimental drought treatment with average values declining from 5.7 mmol m^{-2} s^{-1} on Day 0 to 0.33 mmol m^{-2} s^{-1} on Day 1. These low leaf transpiration values continued through Days 4 and 7. The strong reduction in g_s, A, and E observed during on Days 1, 4, and 7 in drought-treated individuals was associated with

12

a decrease in leaf water potential (*LWP*). Average *LWP* declined from -0.56 MPa in drought-treated leaves on Day 0 to -1.0 on Days 1, 4, and 7, representing a 79% decline. After the drought treatment, despite daily soil moisture additions resuming for the droughted trees, all the trees lost their leaves.

Branch MeOH and AA emission responses to experimental drought

During the drought experiment, a subset of drought (N = 6) and control (N = 6) plants were transported to the analytical laboratory in the morning and analyzed for 'snap-shot' branch MeOH and AA emissions for 1 hour in a constant light and temperature environment (**Fig. 2a-c**). Control plants had high average rates of MeOH emissions (2.3-4.4 nmol m^{-2} s^{-1}) and low, but detectable levels of AA emissions (0.1 nmol m^{-2} s^{-1}). In contrast, drought-stressed trees showed low MeOH emissions (0.3 nmol m^{-2} s^{-1}) while also showing higher average AA emissions (0.2 nmol m^{-2} s^{-1}). This pattern resulted in lower branch 'snap-shot' AA/MeOH emission ratios for the control plants (10 +/- 10%) relative to drought stressed plants (84 +/- 57%).

In contrast to greenhouse drought experiments which showed rapid negative leaf physiological effects, a second set of drought experiments occurred in a cooler lab, where artificial lighting was provided and gas exchange fluxes from a canopy branch were continuously monitored. While variability in the timing and magnitudes of the MeOH and AA emissions was observed between the five individuals, the same general emission pattern was observed during the real-time emission studies as those from the 'snap-shot' studies with drought inducing a pattern of

13

296 decreasing branch MeOH emissions and increasing AA emissions together with high AA/MeOH
297 emissions ratios (**Figure 2d-f, Figure 3** and supplementary **Figures S2-5**).
298
299 When the temporal patterns of branch gas exchange during drought was analyzed in more detail,
300 four distinct phases could be described. The first 'growth phase' with physiologically active
301 foliage is characterized by high rates of transpiration, net photosynthesis, and MeOH emissions,
302 with low AA emissions. High MeOH emissions relative to AA emissions from physiologically
303 active branches in the 'growth phase' constrain daytime AA/MeOH emission ratios to low
304 values, reaching maximum mid-day values of 6% (e.g. day 3 in **Figure 3**). The second phase of
305 drought response consists of a strong suppression in MeOH emissions, apparently occurring
306 prior to any reductions in stomatal conductance and CO_2 and H_2O gas exchange (e.g. day 4).
307 Although AA emissions remained low, branch AA/MeOH emission ratios during this 'MeOH
308 suppression' phase increased slightly from 18% on day 4 to 24% on day 5. The third phase of
309 drought response is characterized by a reduction in transpiration and net photosynthesis rates, a
310 continued strong suppression of MeOH emissions, together with high branch emissions of the
311 fermentation volatiles acetaldehyde, ethanol, acetic acid (AA), and acetone (e.g. initiated on day
312 5 in **Figure 3**). High rates of fermentation VOC emissions were found to be initiated both during
313 the day and the night, depending on the individual (**Supplementary Figs. S2-S5**). Emissions of
314 acetaldehyde during this 'fermentation phase' phase was far higher than those of the other
315 fermentation VOCs whose emissions generally tracked acetaldehyde. Elevated branch
316 fermentation VOC emissions continued for three days, with the peak in AA/MeOH emission
317 ratio (444%) occurring on day 6. Throughout this 'fermentation phase', daytime transpiration

14

and net photosynthesis continued to decline. During the final 'senescence phase' (day 7-10), likely associated with irreversible damage to cellular components including photosynthetic membranes, isoprene emissions were suppressed, while AA/MeOH emission ratios declined, remaining high and reaching a value of 50% by day 10.

To test for the potential reversibility of the suppression of branch MeOH emission during drought, when a drought-stressed potted tree showed strong suppression of MeOH emissions in the laboratory, re-watering of the soil with 100 ml additions on day 4 (red arrows in supplementary **Figure S6**), resulted in a rapid (~15 min) return of high branch MeOH emissions and a dramatic reduction of the AA/MeOH emission ratios to around 1%. As the soil continued to dry through the experiment, the suppression of MeOH emissions was again rapidly relieved by a 100 ml soil moisture addition, regardless of whether it was added during the day or night. This effect of water addition on droughted plants, completely altered the normal diurnal cycle in MeOH emissions which normally peak around mid-day in well-watered individuals. Maximum AA/MeOH emission ratios were 12% which were lower than those from branches of the five trees for which water was completely withheld (**Figure 3** and **S2-5**) which showed high maximum AA/MeOH emission ratios ranging from 400-3500%.

Leaf MeOH and AA emission responses to CO_2, light, and temperature

In order to evaluate the effect of environmental conditions on well hydrated poplar branches at the leaf level, MeOH and AA emissions, AA/MeOH ratio, stomatal conductance (g_s), transpiration, and net photosynthesis (P_{net}) measurements occurred in parallel during CO_2, light,

15

and temperature leaf response studies. To minimize leaf water stress, poplar branches were detached, recut under water, with the target leaf placed in the chamber and the rest of the branch placed in a hydrated atmosphere in the dark. In this way, leaf hydration was maximized by shutting down transpiration from all leaves on the branch except the leaf inside the dynamic leaf chamber. Across the CO_2 (A_{net}-C_i, **Figure 4a-c**), light (A_{net}-PAR, **Figure 4d-f**), and temperature (A_{net}-leaf temp., **Figure 4g-i**) response curves, MeOH and AA emissions generally tracked patterns of g_s and E, and did not appear to be strongly dependent on A_{net}. During the C_i response curves, MeOH emissions tended to increase at low C_i and decrease at high $C_{i,}$ together with g_s. During the light curves, g_s values remained high and increased only slightly as a function of PAR, while MeOH and AA emissions also remained relatively stable. In contrast, as leaf temperature increased, g_s declined considerably at high leaf temperature (e.g. above 35°C), while MeOH and AA emissions together with transpiration generally increased up to the highest leaf temperatures (40 °C). While g_s continued to decline in the dark at 40 °C, leaf dark respiration caused A_{net} to quickly drop to negative values. In contrast, MeOH and AA emissions did not show a fast decline in the dark, but rather declined more gradually together with g_s and E. Importantly across C_i and PAR response curves, leaf AA/MeOH emission ratios remained relatively stable with maximum values < 10%. In contrast, AA/MeOH emission ratios increased slightly as a function of temperature reaching maximum values in the light at 40 °C of 10-20%.

Temperature sensitivities of MeOH and AA emissions and AA/MeOH emission ratios from physiologically active trees, detached stems and leaves, hydrated AIR, and whole ecosystems

16

To better understand the role of temperature in enhancing AA/MeOH emission ratios, the sensitivity of MeOH and AA production to air temperature was characterized using branches of well-watered poplar trees, detached stems and leaves, and whole ecosystems. Well-watered poplar trees were individually placed in a growth chamber with diurnally changing air temperature (**Figure 5**). At night in the dark (20:00-6:00), considerable branch transpiration was observed together with relatively high MeOH emissions, and low to undetectable AA emissions. Under constant daytime (6:00-20:00) light conditions, net positive CO_2 assimilation occurred. As observed at the leaf level, branch transpiration together with MeOH and AA emissions were strongly coupled to the diurnal pattern of air temperature, reaching maximum fluxes during the early afternoon peak in air temperature of 27 ºC at 14:00. MeOH emissions were greater than AA emissions at all air temperatures by roughly a factor of 10, except for 1 hour following light to dark transitions where a short burst in AA emissions were observed. Outside of this light-dark period, branch AA/MeOH emission ratios remained low and increased with air temperature up to ~12% (**Figure 5**). High temperature sensitivity of MeOH and AA emissions from detached poplar stem segments in the dark was also observed (Supplementary **Figure S7**). Similar temperature sensitivities of MeOH and AA emissions were also obtained from hydrated whole leaf cell wall preparations (alcohol insoluble residue, AIR). Gas-exchange analysis under controlled temperature with hydrated AIR in porous Teflon tubes showed rapid equilibration of MeOH and AA emissions within 10 min of reaching the new chamber temperature in the dark. MeOH and AA steady state emissions from hydrated AIR samples increased as a function of temperature from 30-50 ºC (**Figure 6**) and were completely dependent on the presence of liquid water interacting with AIR (data not shown). Similar to physiologically active leaves (**Figure 4**),

17

branches (**Figure 5**), and detached stems (Supplementary **Figure S7**), emissions from hydrated AIR were dominated by MeOH with AA/MeOH emission ratios increasing slightly with temperature but remaining below 30%.

In contrast, AA/MeOH emission ratios from drought stressed poplar branches reached high values ranging from 400-3,000% (**Figures 2-3, Supplementary Figures S2-S5**). Similarly, detached poplar leaves placed into the temperature-controlled chamber in the dark in a dry air stream, showed a similar pattern of suppressed MeOH emissions together with temperature stimulated emissions of the fermentation volatiles acetaldehyde, ethanol, acetic acid, and acetone (**Figure 7**). Acetaldehyde emissions peaked at 42.5 ºC, AA emissions peaked at 47.5 ºC, and the AA/MeOH emission ratio reached a maximum of 2,500% at 45 ºC.

When this analysis was applied to previously published datasets at the ecosystem scale during the growing season, average ecosystem emission rates of AA and MeOH (Belgium) and ambient concentrations (Belgium, Alabama, and California) showed clear diurnal patterns closely tracking air temperature. Moreover, ecosystem AA/MeOH emission and concentration ratios increased linearly as a function of air temperature, peaking in the afternoon (Supplementary **Figures S8-9**). The diurnal increase in MeOH/AA concentration ratios in California and Alabama remained below 30%, suggesting that drought conditions were not experienced by the ecosystems.

Changes in cell wall composition and esterification patterns in response to drought stress

18

In order to investigate the potential source(s) of MeOH and AA emissions from poplar leaves and evaluate potential impacts of drought stress on the cell wall polysaccharide composition, leaf bulk monosaccharide composition was determined from AIR samples. Consistent with the expected high pectin content of rapidly expanding leaf primary cell walls, monosaccharide content of AIR from poplar leaves was dominated by galacturonic acid (GalA, **Figure 8a**). While the monosaccharide content, and by extension polysaccharide content of the cell walls remained largely unchanged during drought, we observed an increase in *O*-acetyl ester content during drought (**Figure 8b**). AIR from control leaves released an average of 0.69 μg g^{-1} of free acetate following saponification which increased by 10% to 0.76 μg g^{-1} of free acetate g^{-1} from drought stressed leaves. Leaf AIR *O*-acetyl ester content increased throughout the drought, reaching a maximum after 7 days (**Figure 8b**).

Evaluating acetate in the transpiration stream as a substrate for cell wall O-acetylation

In order to evaluate potential mechanisms involving rapid changes in cell wall *O*-acetylation in response to drought stress, experiments investigating the transport of doubly ^{13}C-labeled $^{13}C_2$-acetate in the transpiration stream of detached branches and a whole intact tree were carried out. To evaluate leaf cell wall *O*-acetylation responses to $^{13}C_2$-acetate in the transpiration stream, cell wall preparations (AIR) were isolated from canopy leaves, and saponified with deuterated sodium hydroxide (NaOD) to quantitatively hydrolyze the esters. The resulting solution was analyzed for acetate isotopologues including monoisotopic acetate ($^{12}C_2$-acetate) and acetate with one (^{13}C-1-acetate, ^{13}C-2-acetate), and two-^{13}C-atoms ($^{13}C_2$-acetate), by one-dimensional ^{1}H-NMR (**Figure 9**).

19

Acetate released upon saponification of the AIR (from 10 mg dried AIR/mL 0.4M NaOD) ranged in concentration between 212-333 nmol/mg AIR (dry wt.), corresponding to 2.12 mM and 3.33 mM. The concentration of acetate in the method blank was 0.006 mM and, to quantify any additional free acetate that may have been present, incubations of AIR in only D_2O were also carried out. Free acetate was only quantifiable in two detached branch leaf samples at (1.2 and 1.4 nmol/mg AIR (dry wt.), or 0.012 mM and 0.014 mM. In the two cases where it was quantifiable, the highest amount of free acetate in the AIR amounted to less than 0.7 % of the total concentration of acetate observed after saponification with 0.4 M NaOD.

The isotopologue distributions were determined from the experimental spectra (**Figure 9**) by integrating the peak areas corresponding to each isotopologue and dividing by the sum of the integrated areas of all acetate peaks. The results are summarized in **Table 1** as the fraction of isotopologue divided by its expected fraction at natural abundance wherein a value of 1 indicates no change. In leaf cell AIR, there was an increase in the $^{13}C_2$-acetate isotopologue by a factor of 125 +/- 31 above its expected fraction at natural abundance along with concomitant decreases in the fractions corresponding to the remaining isotopologues. For example, no significant changes or slight decreases were detected in the relative abundances of mono-labeled ^{13}C-1-acetate and ^{13}C-2-acetate isotopologues. An increase in the fraction of $^{13}C_2$-acetate isotopologue by a factor of 48 +/- 7 was also observed in two of the three canopy leaf samples collected following one week of 10 mM $^{13}C_2$-acetate solution continuously injected into the xylem of an intact potted tree.

20

449

450 During branch and whole tree labeling with $^{13}C_2$-acetate, plant emission data was collected for
451 three different isotopologues of acetic acid in real-time using PTR-MS including $^{12}C_2$-AA, ^{13}C-1-
452 AA + ^{13}C-2-AA, and $^{13}C_2$-AA. During the whole tree labeling with $^{13}C_2$-acetate via the
453 transpiration stream, significant branch emissions of $^{13}C_2$-AA were not observed. However, leaf
454 emissions of $^{13}C_2$-AA could be observed in some of the detached branch experiments (e.g.
455 supplementary **Figure S8**), confirming the delivery of the labeled acetate to the leaves.

456

457 **Discussion**

458 ***Pectin, Methanol, and the Growing Plant Cell Wall***

459 The polysaccharide pectin can account for up to 35% of the primary cell wall in dicots and non-
460 grass monocots, and up to 5% of wood tissues (Mohnen, 2008). Newly synthesized pectin in the
461 primary cell wall is known to be highly methyl esterified, with changes in the degree of pectin
462 methylesterification mediated by pectin methylesterases (PME) known to regulate cell wall
463 mechanical properties like elasticity. The degree of pectin methylesterification can have
464 profound impact on physiological processes like tissue morphogenesis and growth as well as
465 numerous biological functions (Levesque-Tremblay *et al.*, 2015). Cell wall synthesis is coupled
466 to changes in cell wall elasticity mediated by pectate formation following pectin
467 demethylesterification (Peaucelle *et al.*, 2012). In *Arabidopsis*, increases in tissue elasticity in
468 living meristems correlated with pectin demethylesterification (Peaucelle *et al.*, 2011) which is
469 required for the initiation of organ formation (Peaucelle *et al.*, 2008). When pectin demethylation
470 was inhibited, stiffening of the cell walls throughout the meristem was observed which
471 completely blocked the formation of primordia (Peaucelle *et al.*, 2008). Thus, pectin

21

demethylation is a critical process that regulates the direction and speed of cell wall expansion during growth and morphogenesis (Braybrook *et al.*, 2012). Consistent with the view that MeOH emissions from plants into the atmosphere primarily derive from pectin demethylation, numerous studies have revealed that leaf methanol emissions tightly correlate with leaf expansion rates (Hüve *et al.*, 2007) with young rapidly expanding leaves emitting higher fluxes of MeOH than mature leaves (Jardine *et al.*, 2016). Our temperature-controlled gas exchange observations of hydrated leaf bulk cell walls (AIR) provide new direct evidence for pectin demethylation as the dominant source of foliar MeOH emissions. The observations suggest that in addition to enzymatic hydrolysis reactions catalyzed by esterase enzymes within the cell wall, temperature stimulated non-enzymatic hydrolysis of cell wall methyl and *O*-acetyl esters may be an important source of MeOH and AA production *in situ*. Purified whole leaf cell walls (AIR) hydrated and placed in a porous Teflon tubes permitting gas exchange showed remarkably similar temperature sensitivities of MeOH and AA emissions (**Figure 6**) as physiologically active leaves (**Figure 4**), branches (**Figure 5**), detached stems (supplementary **Figure S7**), and whole ecosystems (supplementary **Figures S8**-**9**), confirming plant cell walls as an important source of MeOH and AA emissions.

In contrast to growth processes, abiotic stress responses may be associated with increased cell wall fortification through a reduction in pectin demethylation rates mediated by pectin methyl esterase inhibitors (PMEI). For example, abiotic stress may lead to the inhibition of pectin demethylation via enhanced expression of PMEI genes known to be involved in abiotic stress tolerance (An *et al.*, 2008; Hong *et al.*, 2010; Ren *et al.*, 2019; Wang *et al.*, 2020a). Recent work

22

494 on drought response of leaf-succulent *Aloe vera* reported the drought-induced folding of
495 hydrenchyma cell walls involves changes in pectin esterification (Ahl *et al.*, 2019). It was
496 hypothesized that the cell wall folding process during drought may be initiated by a reduction in
497 pectin de-esterification and its associated MeOH production and Ca^{+2}-complexation, thereby
498 releasing internal constraints on the cell wall. Thus, we suggest that the strong decrease in
499 observed foliar MeOH emissions during water stress (**Figs. 2**,**3**,**7**, supplementary **S2-5**) may be
500 related to both g_s reductions and reduced cell wall de-methylation rates related to increased
501 PMEI activity. We speculate that reductions in tissue water potential leads to the inhibition of
502 pectin methyl ester hydrolysis, MeOH production, and growth.
503
504 Results from the leaf-level environmental response curves (**Figure 4**) are consistent with the
505 view that stomatal regulated leaf MeOH emissions are controlled by light-independent, but
506 highly temperature-dependent production associated with growth processes (Harley et al, 2007).
507 Thus, light and CO_2 are assumed to only indirectly influence leaf MeOH emission rates via
508 changes to g_s. However, we highlight that reduction of g_s at high temperatures in well hydrated
509 leaves was often unable to prevent the temperature increase in MeOH and AA emissions (**Figure**
510 **4**). Similarly, reductions in g_s during drought were unable to suppress the emissions of
511 fermentation volatiles like AA (**Figs. 2**,**3**, supplementary **S2**-**5**). Although a link with g_s is
512 possible, our observations suggest that the large changes in AA/MeOH ratios during growth and
513 drought stress responses are largely due to changes in production rates, with MeOH production
514 declining and AA production increasing during different phases of the drought response (**Figure**
515 **3**). Our study suggests that there are at least two distinct plant sources of atmospheric AA

23

emissions; hydrolysis of *O*-acetyl groups on the cell wall (**Figure 6**) and the aerobic fermentation pathway (**Figures 3, 7**). The metabolic origin of AA is further discussed in the **Supplementary discussion**.

Cell wall O-acetylation is modified by drought

In this study, we found statistically significant enrichments in *O*-acetyl ester content of bulk leaf cell walls (AIR) in response to drought stress (**Figure 8b**). In contrast, cell wall monomer composition, which was dominated by galacturonic acid from pectin, changed little over seven days following the cessation of watering (**Figure 8a**). That leaf AIR monosaccharide content was largely insensitive to drought suggests a slower turnover in monosaccharide cell wall polysaccharides than the fast time scales of days observed for changes in volatile emission signatures and cell wall *O*-acetyl ester content changes (1-7 days). *O*-acetyl-substituents are present on nearly all cell wall polymers with the exception of cellulose, whereas methyl esters are thought to be primarily associated with pectin (Derbyshire *et al.*, 2007). *O*-acetyl esterification of plant cell walls is known to play important physicochemical, mechanical, and structural roles that serve to minimize degradation while enhancing intermolecular interactions with other wall polymers (Biely, 2012). Studies have shown that cell wall *O*-acetylation of hemicellulose and pectin is critical for proper plant growth and functioning. For example, simultaneous mutations of the acetyl transferase genes *TBL32*, *TBL33* and *TBL29*/*ESK1* in *Arabidopsis* resulted in a severe reduction in xylan *O*-acetyl level down to 15% that of the wild type, and concomitantly, severely collapsed vessels and stunted plant growth (Yuan *et al.*, 2016). Likewise, strongly reduced growth and collapsed vessels were found in *Arabidopsis* mutated in

24

the four *Reduced Wall Acetylation* (*RWA*) genes, which may encode Golgi-localized transporters of substrates for acetyl transferases (Manabe et al. 2013). Additional studies demonstrated that *Arabidopsis* plants with defective TBL29/ESK1 enzymes have a constitutive drought syndrome and collapsed xylem vessels, low hydraulic conductivity along with low *O*-acetylation levels in xylan and mannan, low transpiration rates, high water use efficiency, and dwarfism (Lefebvre *et al.*, 2011; Ramírez *et al.*, 2018). Together with these studies, the observation of enhanced leaf cell wall *O*-acetylation during drought (**Figure 8b**) suggests that polysaccharide *O*-acetylation is important for the proper functioning of vascular tissues under water deficit.

Acetate as a potential substrate for cell wall O-acetylation

While the mechanisms of methyl esterification of pectin and its de-methylation by PME have been the focus of several studies (Willats *et al.*, 2001; Mohnen, 2008), the mechanisms of how *O*-acetyl groups are transferred to and from cell wall polymers and their role in the life cycle of a plant are poorly understood. Current biochemical models of cell wall esters assume that carbohydrate monomers are heavily *O*-acetylated using acetyl-CoA or another acetyl donor initially in the Golgi apparatus, and subsequently exported and incorporated into the growing cell wall. The wall polymers can then be de-esterified in the wall by esterase enzymes at a later point in the life cycle of the cell in support of numerous physiological and biochemical processes. Acetyl transfer activity from acetyl-CoA to xylooligomer acceptors has been attributed to Golgi localized TBL acetyl transferases (Urbanowicz et al. 2014; Zhong *et al.*, 2017). Notably, acetyl donors such as *p*-nitrophenyl acetate and acetyl salicylic acid are even better substrates for TBL29 in vitro than acetyl-CoA (Lunin et al., 2020), and transport of acetyl CoA into the Golgi

25

lumen has not been demonstrated. Hence, it is possible that the immediate donor for cell wall acetylation is not acetyl CoA but an unknown acetyl donor, although it may be generated from acetyl CoA. We observed that delivery of $^{13}C_2$-acetate to the transpiration stream of poplar branches and xylem of a whole tree leads to rapid and significant $^{13}C_2$-labeling of *O*-acetyl esters in isolated leaf cell walls (AIR). Therefore, activation of $^{13}C_2$-acetate to $^{13}C_2$-acetyl-CoA or an unidentified acetyl donor utilized by Golgi-localized acetyl transferases could explain the $^{13}C_2$-labeling of *O*-acetyl esters observed in leaf cell walls isolations (AIR) (**Table 1**). ^{1}H-NMR analysis of the acetate released following leaf AIR saponification show that satellite signals corresponding to the $^{13}C_2$-acetate isotopologue were detectable in all three detached branch leaf AIR samples and two of the three whole tree leaf AIR samples which had been treated with 10 mM $^{13}C_2$-acetate via the transpiration stream. In contrast, AIR of leaves labeled with $^{13}C_2$-acetate treated with water instead of NaOD did not show any detectable $^{13}C_2$-acetate in solution, suggesting the acetate was bound to the cell wall material via an ester bond, making it unlikely that the delivered $^{13}C_2$-acetate in the transpiration stream became trapped in the cell wall material, but not esterified.

These results suggest a possible link between the drought-induced increase in foliar AA emissions (e.g. **Figure 3**) and increased *O*-acetylation of leaf cell walls (**Figure 8b**). Thus, in addition to providing acetate for protein acetylation and defense gene regulation (Kim et al., 2017), the activation of aerobic fermentation during drought may also supply acetyl-CoA used in the Golgi prior to incorporation into the cell wall (Gou et al., 2012; Orfila et al., 2012; de Souza et al., 2014). This hypothesis is consistent with previous studies with microsomal preparations of

26

582 a potato cell suspension culture that were supplied with ^{14}C-acetyl-CoA found radio-labeled
583 acetate in an esterified form on several polysaccharides, including xyloglucan and pectin (Pauly
584 and Scheller, 2000). Although the mechanisms require further investigation, our study is
585 consistent with cell wall methylation and *O*-acetylation of polysaccharides rapidly responding to
586 environmental conditions, potentially allowing plants the flexibility to dynamically alter growth
587 and defense processes. Our observations are consistent with a coordinated reduction in cell wall
588 de-methyl esterification and growth processes during water stress (resulting in a strong
589 suppression in MeOH production) together with an activation of defense processes including
590 stomatal closure, aerobic fermentation (increasing AA production and emissions), and
591 enhancements in cell wall *O*-acetylation.
592
593 **Conclusions and prospects**
594 Although plants are known to activate growth suppression and defense signaling during abiotic
595 stress, the biochemical, physiological, and ecological mechanisms involved are under intense
596 investigation. In this study, we identified the active growth phase associated with rapid biomass
597 accumulation and high rates of leaf gas exchange as highly enriched in MeOH emissions relative
598 to AA. AA and MeOH emission patterns of hydrated leaf cell wall isolations (AIR) showed
599 similar temperature sensitivities when compared with physiologically active poplar leaves,
600 branches, and ecosystems. The striking similarities in temperature sensitivities of AA/MeOH
601 emissions from AIR, leaves, branches, and whole ecosystems provides direct evidence for the
602 cell wall as the main source of foliar MeOH and AA emissions during normal physiological
603 activities. However, drought exposure led to large increases in AA/MeOH emissions (400-
604 3,500%) linked to numerous coordinated leaf physiological and biochemical changes starting

27

with a suppression of MeOH emissions followed by a suppression of net photosynthesis and transpiration, a large increase in foliar AA emissions, and increase in cell wall *O*-acetylation. While the metabolic origin of AA under drought stress requires further evaluation, we suggest that AA/MeOH emission ratios may be exploited by future plant and ecosystem studies as a highly sensitive atmospheric signal reflecting growth-defense trade-offs in plants and ecosystems as they move between optimal growth conditions and abiotic stress associated with decreased productivity.

Supplementary Information

The following supplementary methods and data are available online

Supplementary Information Content

28

- **Figure S8**: Average diurnal MeOH and AA ambient concentrations and (**b**) vertical fluxes together with air temperature above a poplar plantation during the 2015 growing season in Belgium (Portillo-Estrada *et al.*, 2018)
- **Figure S9**: Average diurnal MeOH and AA concentrations and AA/MeOH ratios together with air temperature during the growing season above (**a**) a mixed forest in Alabama, USA (Su *et al.*, 2016) and (**b**) a citrus grove in California, USA (Park *et al.*, 2013) during the growing season. Average diurnal MeOH (blue) and AA (green) ambient concentrations with air temperature together with AA/MeOH concentration ratios are plotted.
- **Figure S10**: Leaf $^{13}C_2$-acetic acid emissions during branch $^{13}C_2$-acetate labeling via the transpiration stream

Supplementary References

29

Leaf sample	Acetate isotopologue	$F_{experiment}/F_{natural\ abundance}$
Detached branch	$^{12}C_2$-acetate	0.985 +/- 0.008 (*)
Detached branch	^{13}C-1-acetate	0.6 +/- 0.3 (ns)
Detached branch	^{13}C-2-acetate	1.00 +/- 0.09 (ns)
Detached branch	$^{13}C_2$-acetate	125 +/- 31 (*)
Whole tree	$^{12}C_2$-acetate	0.995 +/- 0.004 (ns)
Whole tree	^{13}C-1-acetate	0.9 +/- 0.2 (ns)
Whole tree	^{13}C-2-acetate	1.01 +/- 0.04 (ns)
Whole tree	$^{13}C_2$-acetate	48 +/- 7 (*)

Table 1. ^{1}H-NMR isotopologue analysis results for acetate released following saponification of isolated leaf cell wall samples from (**a**) 3 detached branches (one per tree, N = 3) treated with 10 mM $^{13}C_2$-acetate solution for 2 days as well as (**b**) canopy leaf (N = 3) samples from a 2-year old tree following continuous diurnal injections of the 10 mM $^{13}C_2$-solution into the xylem at the base of the tree for 7 days (night: 70 µL/min, day: 150 µL/min). Following saponification of the cell wall isolates, the values were obtained by integrating the area of the free acetate signals (corresponding to each of the four isotopologues shown in **Fig. 10**), and calculating the fraction ofeach acetate isotopologue to the total ($F_{experiment}$ = peak area acetate isotopologue/peak area of total acetate isotopologues), and reporting the ratio of F_{exp} to that from natural abundance fractions ($F_{natural\ abundance}$). Note, statistically significant changes in $F_{experiment}/F_{natural\ abundance}$ (*), no statistically significant changes (ns).

30

Figures

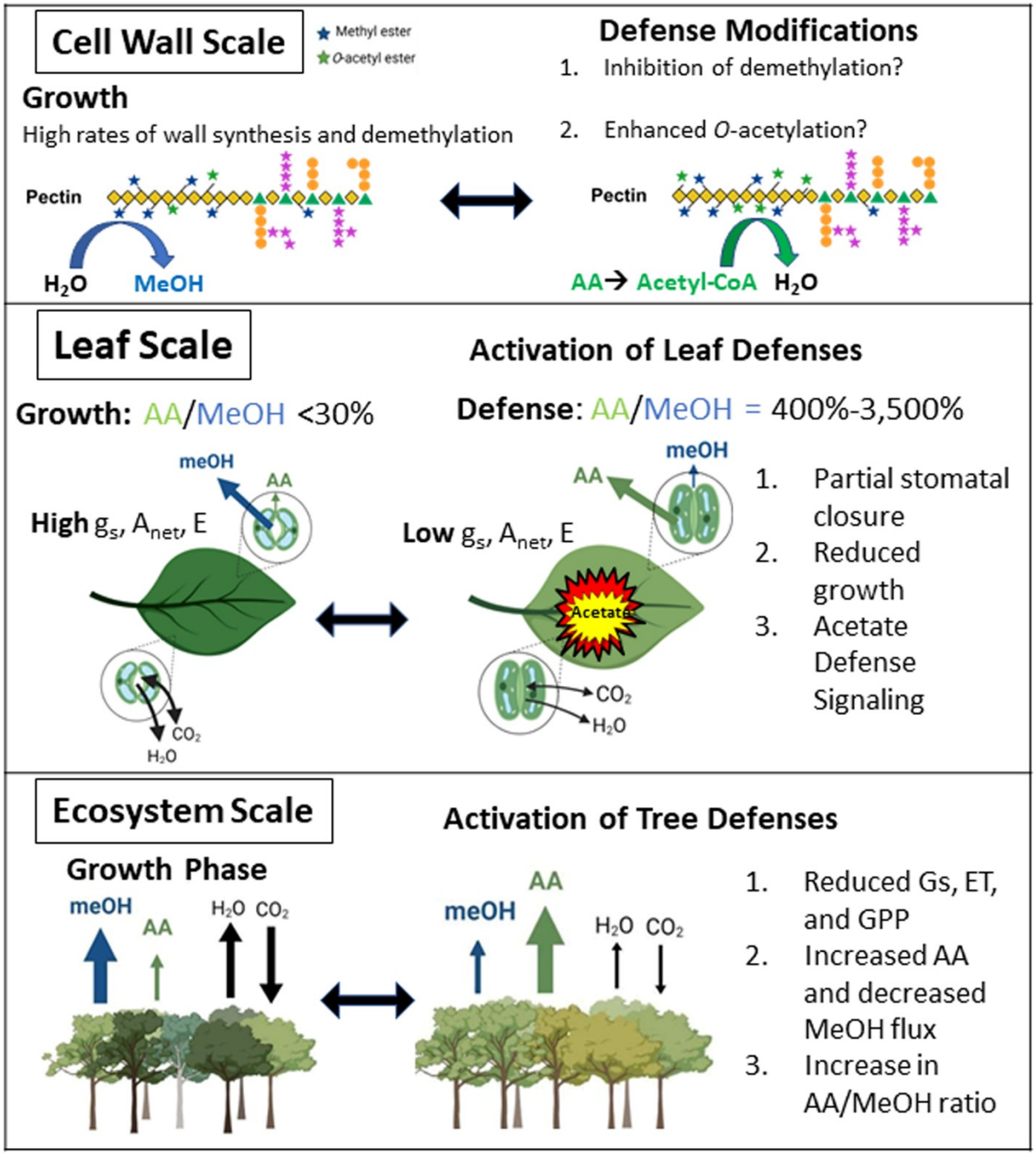

Graphical abstract: Summary of changes to MeOH and AA emission patterns, cell wall *O*-acetylation, and leaf gas exchange in poplar trees during growth and defense against drought stress from cell walls, leaves, to whole ecosystems.

31

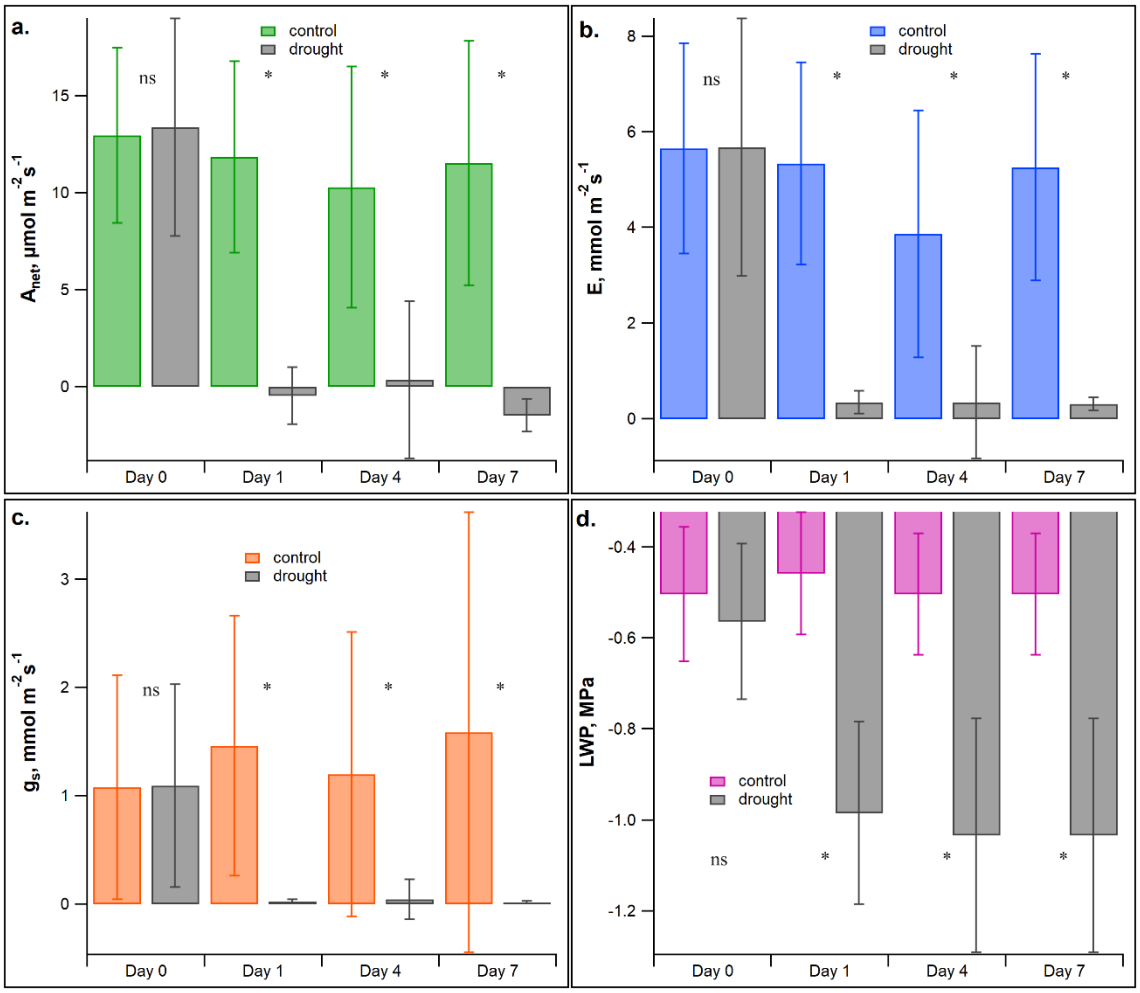

Figure 1: Leaf physiological parameters in control and drought treated plants. Poplar saplings were subject to drought for 7 days. Leaf observations were made on day 0 (n =24), day 1 (n =6), day 4 (n=18), and day 7 (n=18) of (**a**) Net photosynthesis (A_{net}, µmol m^{-2} s^{-1}), (**b**) transpiration (E, mmol m^{-2} s^{-1}), (**c**) stomatal conductance (g_s, mmol m^{-2} s^{-1}) and (**d**) leaf water potential (LWP, MPa). Values are plotted as average +/- 1 standard deviation (ns indicates no statistical significance between control and drought treatments, * indicates statistically significant difference, P <0.05).

32

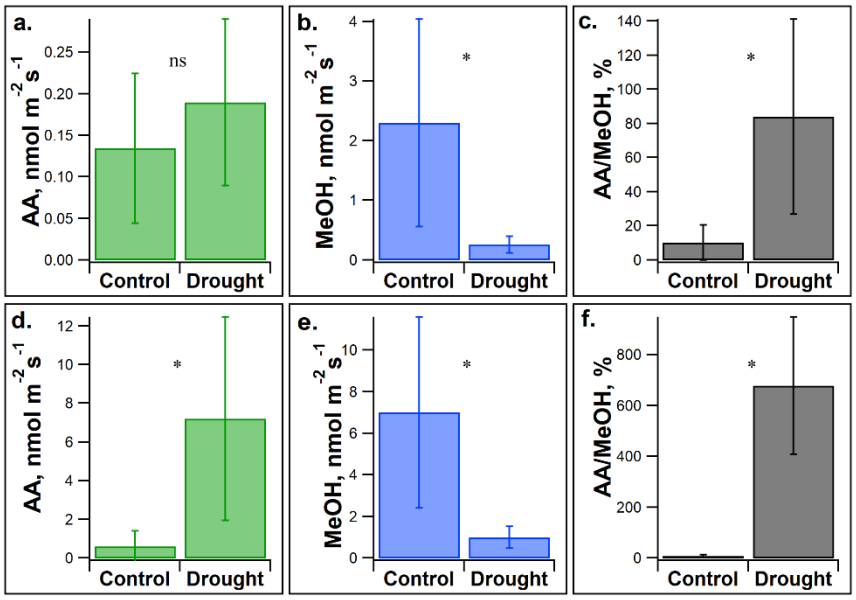

676

677 **Figure 2:** Branch daytime 'snap-shot' branch emissions of (**a**) acetic acid (AA), (**b**) methanol
678 (MeOH), and (**c**) the AA/MeOH emission ratio from control (N = 21) and drought stressed (N =
679 16) poplar trees measured on Day 1 of the drought. In addition, the daily maximum (**d**) AA
680 emissions, (**e**) MeOH emissions, and (**f**) AA/MeOH emission ratios from real-time branch gas
681 exchange measurements on the first day of secession of soil water addition (Day = 0: control)
682 and a subsequent day during the drought response at the time where AA emissions were
683 maximized (N = 5) are also shown. All values are plotted as average +/- one standard deviation
684 (ns indicates no statistical significance between control and drought treatments, * indicates
685 statistically significant differences, $P < 0.05$).

33

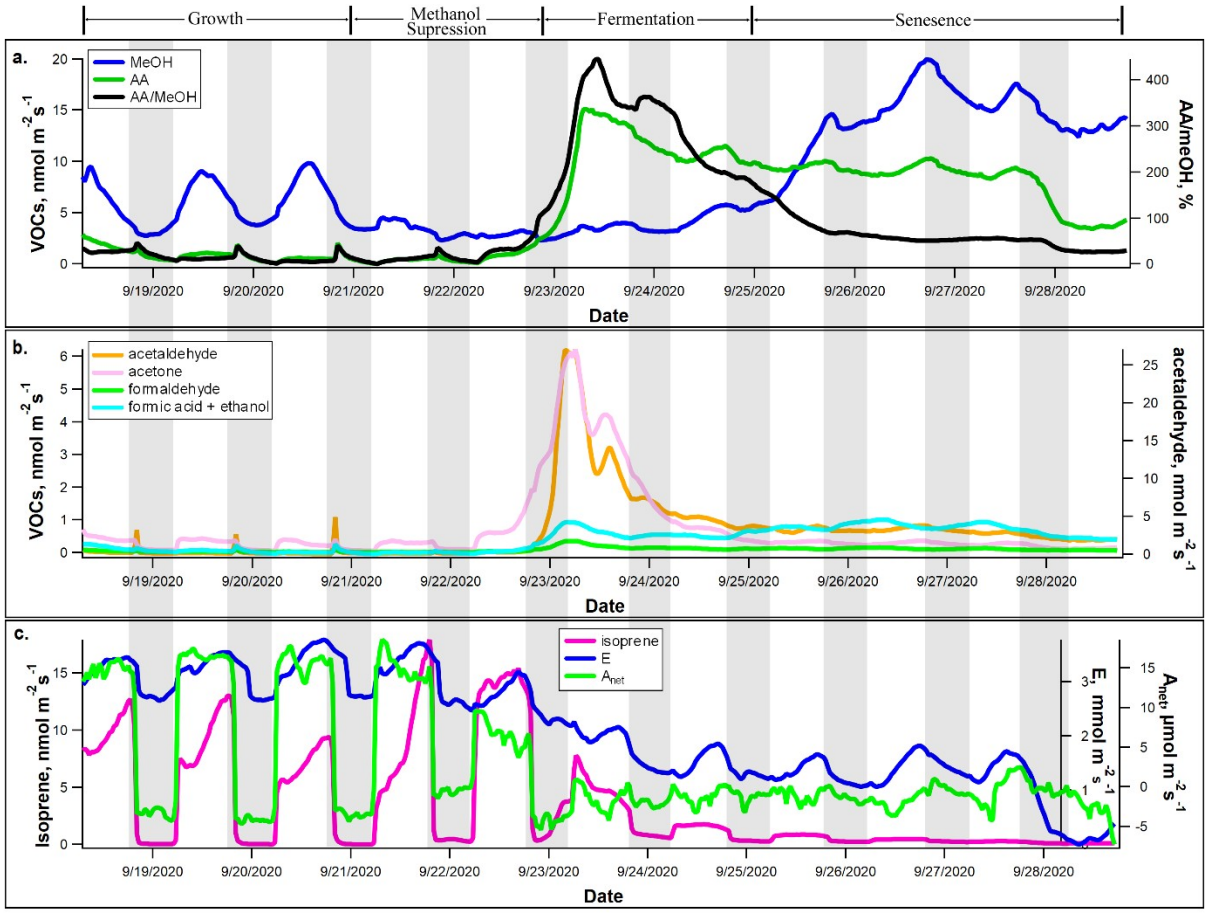

686

687 **Figure 3:** Real-time branch emissions of VOCs together with transpiration (E, mmol m^{-2} s^{-1}) and
688 net photosynthesis (A_{net}, µmol m^{-2} s^{-1}) fluxes during a 10-day drought experiment. A branch
689 enclosure was installed on a potted poplar tree and water withheld for the 10-day duration. Daily
690 branch flux patterns of (**a**) Methanol (MeOH), Acetic Acid (AA), AA/MeOH emission ratio, (**b**)
691 Aerobic fermentation intermediates (acetaldehyde, ethanol, acetone) (**c**) CO_2 and H_2O and the
692 photosynthetic product isoprene. Shaded areas represent the nigh-time where the grow light was
693 switched off.
694

34

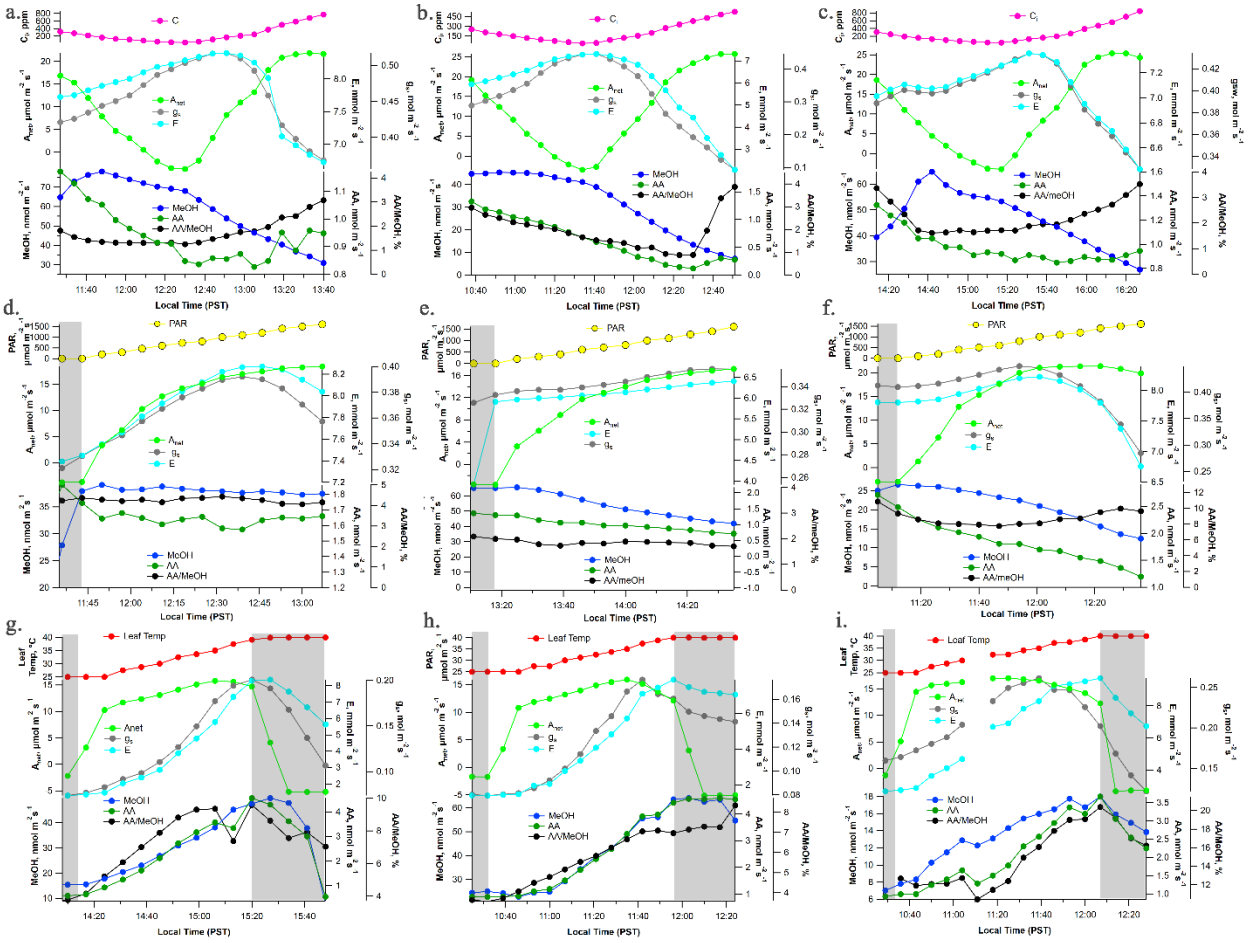

Figure 4: Dynamic leaf gas exchange responses of methanol (MeOH), acetic acid (AA), AA/MeOH, net photosynthesis (A_{net}), transpiration (E), and stomatal conductance (g_s) from detached hydrated poplar branches as a function of (**a-c**) leaf internal CO_2 concentrations (C_i), (**d-f**) incident Photosynthetically Active Radiation (PAR) flux, and (**g-i**) leaf temperature. Shaded regions indicate dark conditions inside the leaf chamber.

35

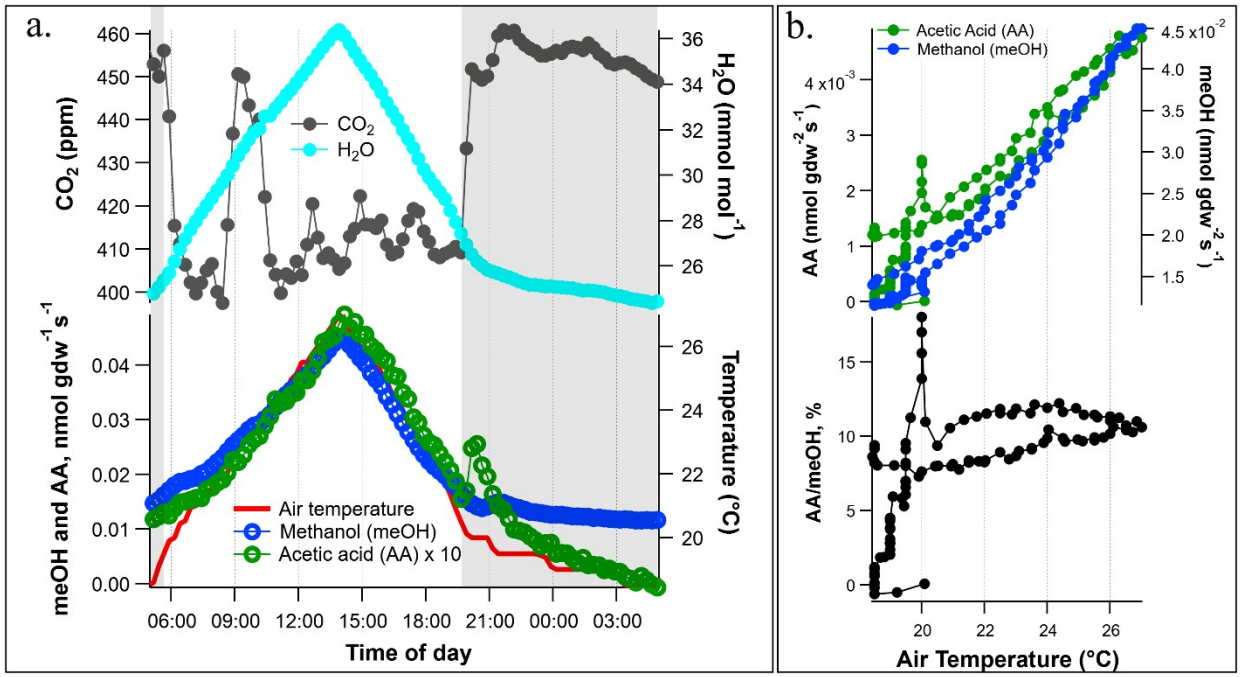

701

702 **Figure 5:** (**a**) Example diurnal pattern of AA and MeOH emissions from a physiologically active
703 poplar branch from a tree inside a growth chamber programmed with a temperature increase
704 during the day under constant illumination. (**b**) Also shown are AA and MeOH emissions and the
705 ratio of AA/MeOH emissions plotted as a function of air temperature. Shaded areas represent the
706 nigh-time where the grow light was switched off.

36

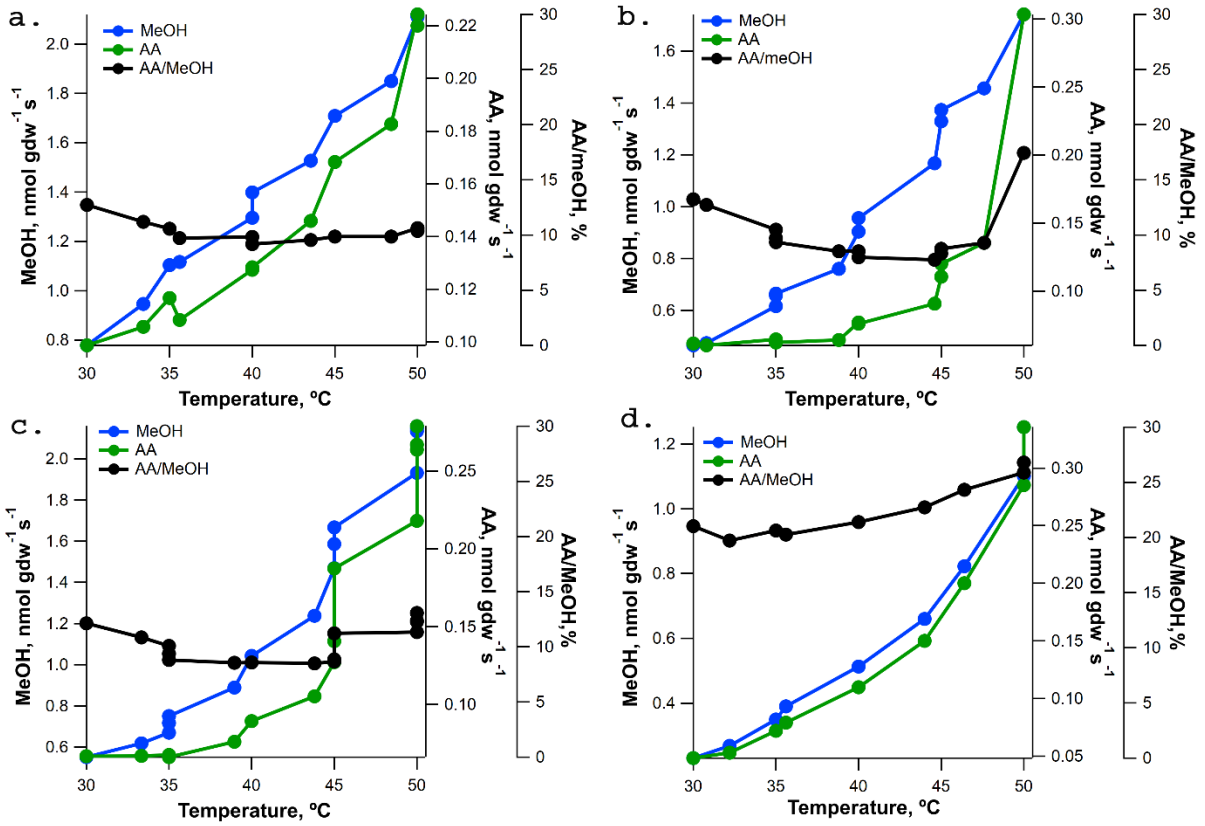

Figure 6: Emissions of methanol (MeOH) and acetic acid (AA) as a function of time from hydrated leaf cell wall isolates (AIR) in porous Teflon PTFE diffusion tubes as chamber air temperature increased from 30 °C to 50 °C.

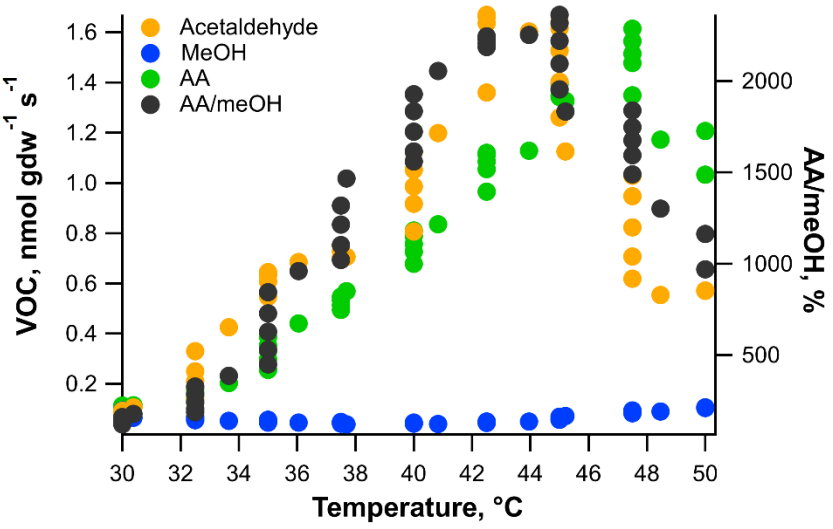

Figure 7: Example Acetaldehyde and Acetic Acid (AA) emissions from a detached poplar leaf in the dark with 1.0 L min dry air passing over in a temperature-controlled chamber (Ethanol and

37

Acetone emissions are not shown for clarity). Average Acetaldehyde, AA, MeOH, and AA/MeOH emission values are plotted at each chamber temperature.

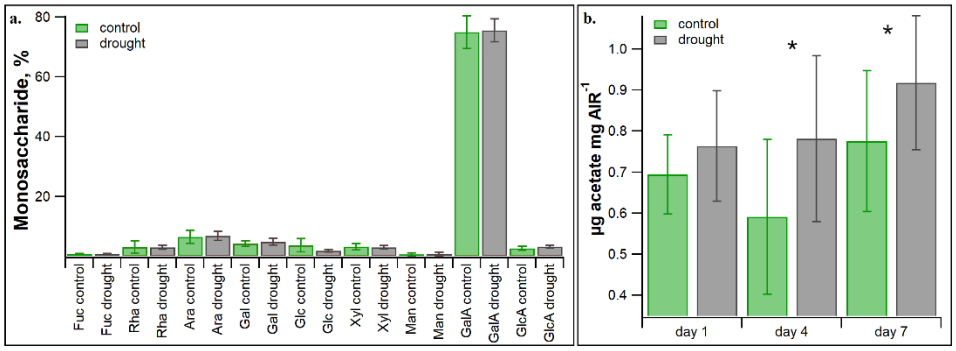

Figure 8: a. Leaf bulk cell wall monosaccharide composition from control and drought stressed poplar trees one day following cessation of soil moisture additions. Monosaccharides quantified are fucose (Fuc), rhamnose (Rha), arabinose (Ara), galactose (Gal), glucose (Glc), xylose (Xyl), mannose (Man), galacturonic acid (GalA) and glucuronic acid (GlcA). **b.** Also shown are leaf bulk cell wall *O*-acetyl methyl ester content released following saponification of alcohol insoluble residue (AIR) preparations from control and drought stressed leaves on day 1, 4, and 7. Values are plotted as average +/- one standard deviation (* indicates statistically significant difference between control and drought treatments, $P < 0.05$). Note, no statistically significant differences were observed in monosaccharide composition between control and drought treatments during days 1,4, or 7.

38

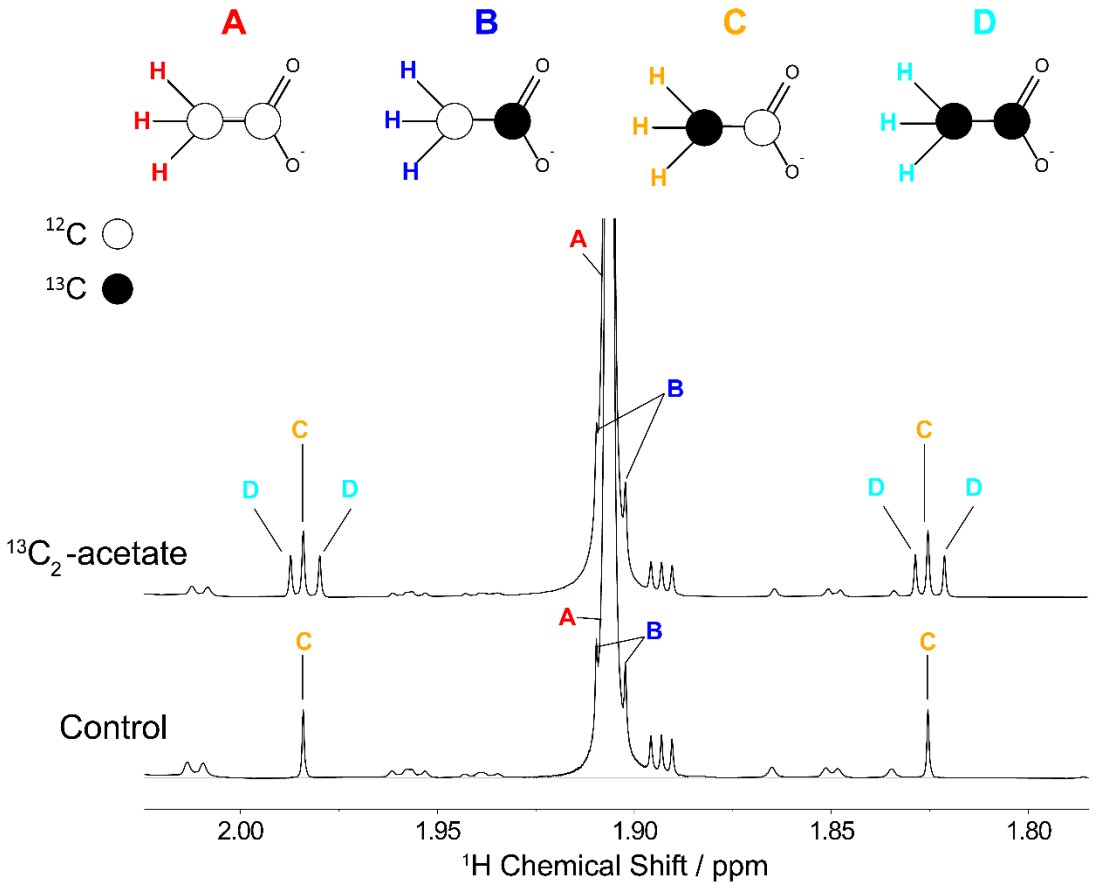

730

731 **Figure 9**: **Exploring the mechanism of leaf bulk cell wall *O*-acetylation.** Simplified schematic
732 showing acetate and its four-stable carbon isotopologues with 0 (**A**), 1 (**B** and **C**), and 2 (**D**) ^{13}C
733 atoms. Following delivery of a 10 mM $^{13}C_2$-acetate to detached poplar branches and a whole
734 poplar tree via the transpiration stream, leaf cell walls were isolated and analyzed by ^{1}H-NMR.
735 Note: the much more intense $^{12}C_2$-isotopologue signal (A) was clipped vertically in both control
736 and $^{13}C_2$-acetate spectra to show the details of the satellite peaks corresponding to the remaining
737 isotopologues which are labeled B-D. The acetate $^1J_{CH}$ = 127.0 +/- 0.1 Hz and the $^2J_{CH}$ = 5.9 +/-
738 0.1 Hz.
739
740
741

39

Acknowledgements

This material is based upon work supported by the U.S. Department of Energy (DOE), Office of Science, Office of Biological and Environmental Research (BER), Biological System Science Division (BSSD), Early Career Research Program under Award number FP00007421 to Lawrence Berkeley National Laboratory. This work was also supported as part of the DOE Joint BioEnergy Institute through contract DE-AC02-05CH11231 to Lawrence Berkeley National Laboratory (LBNL). A portion of this research was performed on project awards (10.46936/cpcy.proj.2019.50708/60006566 and 10.46936/expl.proj.2019.51078/60006676) from the Environmental Molecular Sciences Laboratory, a DOE Office of Science User Facility sponsored by the BER program under Contract No. DE-AC05-76RL01830. We would like to acknowledge extensive project guidance from Eoin Brodie at (LBNL) and Christina Wistrom for the maintenance and establishment of our poplar trees at the UC Berkeley Oxford Greenhouse. In addition, we would like to acknowledge Thomas Powell for practical advice on leaf water potential measurements and the helpful discussions on cell wall elasticity and plant drought stress responses.

References

Ahl L.I., Mravec J., Jørgensen B., Rudall P.J., Rønsted N. & Grace O.M. (2019) Dynamics of intracellular mannan and cell wall folding in the drought responses of succulent Aloe species. *Plant, Cell & Environment* **42**, 2458–2471.

Amsbury S., Hunt L., Elhaddad N., Baillie A., Lundgren M., Verhertbruggen Y., … Gray J.E. (2016) Stomatal Function Requires Pectin De-methyl-esterification of the Guard Cell Wall. *Current Biology* **26**, 2899–2906.

An S.H., Sohn K.H., Choi H.W., Hwang I.S., Lee S.C. & Hwang B.K. (2008) Pepper pectin methylesterase inhibitor protein CaPMEI1 is required for antifungal activity, basal disease resistance and abiotic stress tolerance. *Planta* **228**, 61–78.

40

Aulia M.R., Liyantono, Setiawan Y. & Fatikhunnada A. (2016) Drought detection of west java's paddy field using MODIS EVI satellite images (case study: rancaekek and rancaekek wetan). *Procedia Environmental Sciences* **33**, 646–653.

Biely P. (2012) Microbial carbohydrate esterases deacetylating plant polysaccharides. *Biotechnology advances* **30**, 1575–1588.

Braybrook S.A., Hofte H. & Peaucelle A. (2012) Probing the mechanical contributions of the pectin matrix: insights for cell growth. *Plant Signaling & Behavior* **7**, 1037–1041.

Chebli Y. & Geitmann A. (2017) Cellular growth in plants requires regulation of cell wall biochemistry. *Current Opinion in Cell Biology* **44**, 28–35.

Derbyshire P., McCann M.C. & Roberts K. (2007) Restricted cell elongation in Arabidopsis hypocotyls is associated with a reduced average pectin esterification level. *BMC Plant Biology* **7**, 31.

Dewhirst R.A., Afseth C.A., Castanha C., Mortimer J.C. & Jardine K.J. (2020b) Cell wall O-acetyl and methyl esterification patterns of leaves reflected in atmospheric emission signatures of acetic acid and methanol. *Plos One* **15**, e0227591.

Dewhirst R.A., Handakumbura P., Clendinen C.S., Arm E., Tate K., Wang W., … Jardine K.J. (2021a) High Temperature Acclimation of Leaf Gas Exchange, Photochemistry, and Metabolomic Profiles in *Populus trichocarpa*. *ACS Earth and Space Chemistry*.

Dewhirst R.A., Mortimer J.C. & Jardine K.J. (2020a) Do cell wall esters facilitate forest response to climate? *Trends in Plant Science* **25**, 729–732.

Fall R. (2003) Abundant oxygenates in the atmosphere: a biochemical perspective. *Chemical Reviews* **103**, 4941–4952.

Furtado A., Lupoi J.S., Hoang N.V., Healey A., Singh S., Simmons B.A. & Henry R.J. (2014) Modifying plants for biofuel and biomaterial production. *Plant Biotechnology Journal* **12**, 1246–1258.

Ganie S.A. & Ahammed G.J. (2021) Dynamics of cell wall structure and related genomic resources for drought tolerance in rice. *Plant Cell Reports* **40**, 437–459.

Gille S. & Pauly M. (2012) O-acetylation of plant cell wall polysaccharides. *Frontiers in plant science* **3**, 12.

Gou J.-Y., Miller L.M., Hou G., Yu X.-H., Chen X.-Y. & Liu C.-J. (2012) Acetylesterase-mediated deacetylation of pectin impairs cell elongation, pollen germination, and plant reproduction. *The Plant Cell* **24**, 50–65.

Harley, P., Greenberg, J., Niinemets, Ü. and Guenther, A., 2007. Environmental controls over methanol emission from leaves. *Biogeosciences*, **4**(**6**), 1083-1099.

Helm L.T., Shi H., Lerdau M.T. & Yang X. (2020) Solar-induced chlorophyll fluorescence and short-term photosynthetic response to drought. *Ecological Applications* **30**, e02101.

Hong M.J., Kim D.Y., Lee T.G., Jeon W.B. & Seo Y.W. (2010) Functional characterization of pectin methylesterase inhibitor (PMEI) in wheat. *Genes & Genetic Systems* **85**, 97–106.

Hüve K., Christ M.M., Kleist E., Uerlings R., Niinemets U., Walter A. & Wildt J. (2007) Simultaneous growth and emission measurements demonstrate an interactive control of methanol release by leaf expansion and stomata. *Journal of Experimental Botany* **58**, 1783–1793.

41

Jardine K.J., Chambers J.Q., Holm J., Jardine A.B., Fontes C.G., Zorzanelli R.F., … Manzi A.O. (2015) Green Leaf Volatile Emissions during High Temperature and Drought Stress in a Central Amazon Rainforest. *Plants* **4**, 678–690.

Jardine K.J., Fernandes de Souza V., Oikawa P., Higuchi N., Bill M., Porras R., … Chambers J.Q. (2017) Integration of C_1 and C_2 metabolism in trees. *International Journal of Molecular Sciences* **18**, 2045.

Jardine K.J., Jardine A.B., Souza V.F., Carneiro V., Ceron J.V., Gimenez B.O., … Chambers J.Q. (2016) Methanol and isoprene emissions from the fast-growing tropical pioneer species *Vismia guianensis* (Aubl.) Pers. (Hypericaceae) in the central Amazon forest. *Atmospheric Chemistry and Physics* **16**, 6441–6452.

Jardine K, Yañez Serrano A, Arneth A, Abrell L, Jardine A, Artaxo P, Alves E, Kesselmeier J, Taylor T, Saleska S, Huxman T. (2011) Ecosystem-scale compensation points of formic and acetic acid in the central Amazon. Biogeosciences **8**(**12**), 3709-20.

Ji Y., Zhou G., Li Z., Wang S., Zhou H. & Song X. (2020) Triggers of widespread dieback and mortality of poplar (Populus spp.) plantations across northern China. *Journal of arid environments* **174**, 104076.

Kim J.-M., To T.K., Matsui A., Tanoi K., Kobayashi N.I., Matsuda F., … Seki M. (2017) Acetate-mediated novel survival strategy against drought in plants. *Nature Plants* **3**, 17097.

Lefebvre V., Fortabat M.-N., Ducamp A., North H.M., Maia-Grondard A., Trouverie J., … Durand-Tardif M. (2011) ESKIMO1 disruption in Arabidopsis alters vascular tissue and impairs water transport. *Plos One* **6**, e16645.

Levesque-Tremblay G., Pelloux J., Braybrook S.A. & Müller K. (2015) Tuning of pectin methylesterification: consequences for cell wall biomechanics and development. *Planta* **242**, 791–811.

Liu Y., Zhou R., Wen Z., Khalifa M., Zheng C., Ren H., … Wang Z. (2021) Assessing the impacts of drought on net primary productivity of global land biomes in different climate zones. *Ecological Indicators* **130**, 108146.

Lunin VV, Wang HT, Bharadwaj VS, Alahuhta M, Peña MJ, Yang JY, Archer-Hartmann SA, Azadi P, Himmel ME, Moremen KW, York WS. (2020) Molecular mechanism of polysaccharide acetylation by the Arabidopsis xylan O-acetyltransferase XOAT1. *The Plant Cell* **32**, 2367-82.

Manabe Y, Verhertbruggen Y, Gille S, Harholt J, Chong SL, Pawar PM, Mellerowicz EJ, Tenkanen M, Cheng K, Pauly M, Scheller HV. (2013) Reduced wall acetylation proteins play vital and distinct roles in cell wall O-acetylation in Arabidopsis. *Plant physiology* **163**, 1107-17.

McDowell N., Pockman W.T., Allen C.D., Breshears D.D., Cobb N., Kolb T., … Yepez E.A. (2008) Mechanisms of plant survival and mortality during drought: why do some plants survive while others succumb to drought? *The New Phytologist* **178**, 719–739.

Mohnen D. (2008) Pectin structure and biosynthesis. *Current Opinion in Plant Biology* **11**, 266–277.

Novaković L., Guo T., Bacic A., Sampathkumar A. & Johnson K.L. (2018) Hitting the Wall-Sensing and Signaling Pathways Involved in Plant Cell Wall Remodeling in Response to Abiotic Stress. *Plants* **7**, 89.

42

Orfila C., Dal Degan F., Jørgensen B., Scheller H.V., Ray P.M. & Ulvskov P. (2012) Expression of mung bean pectin acetyl esterase in potato tubers: effect on acetylation of cell wall polymers and tuber mechanical properties. *Planta* **236**, 185–196.
Park J.H., Goldstein A.H. & Timkovsky J. (2013) Eddy covariance emission and deposition flux measurements using proton transfer reaction–time of flight–mass spectrometry (PTR-TOF-MS): comparison with PTR-MS measured vertical gradients and fluxes. *Atmospheric Chemistry and Physics,* **13**, 1439-1456.
Pauly M. & Keegstra K. (2010) Plant cell wall polymers as precursors for biofuels. *Current Opinion in Plant Biology* **13**, 305–312.
Pauly M. & Scheller H.V. (2000) O-Acetylation of plant cell wall polysaccharides: identification and partial characterization of a rhamnogalacturonan O-acetyl-transferase from potato suspension-cultured cells. *Planta* **210**, 659–667.
Peaucelle A., Braybrook S. & Höfte H. (2012) Cell wall mechanics and growth control in plants: the role of pectins revisited. *Frontiers in plant science* **3**, 121.
Peaucelle A., Braybrook S.A., Le Guillou L., Bron E., Kuhlemeier C. & Höfte H. (2011) Pectin-induced changes in cell wall mechanics underlie organ initiation in Arabidopsis. *Current Biology* **21**, 1720–1726.
Peaucelle A., Louvet R., Johansen J.N., Höfte H., Laufs P., Pelloux J. & Mouille G. (2008) Arabidopsis phyllotaxis is controlled by the methyl-esterification status of cell-wall pectins. *Current Biology* **18**, 1943–1948.
Peters A.J., Walter-Shea E.A., Ji L. & Vina A. (2002) Drought monitoring with NDVI-based standardized vegetation index. … *and remote sensing*.
Portillo-Estrada M., Zenone T., Arriga N. & Ceulemans R. (2018) Contribution of volatile organic compound fluxes to the ecosystem carbon budget of a poplar short-rotation plantation. *Global change biology. Bioenergy* **10**, 405–414.
Ragauskas A.J., Williams C.K., Davison B.H., Britovsek G., Cairney J., Eckert C.A., … Tschaplinski T. (2006) The path forward for biofuels and biomaterials. *Science* **311**, 484–489.
Ramírez V., Xiong G., Mashiguchi K., Yamaguchi S. & Pauly M. (2018) Growth- and stress-related defects associated with wall hypoacetylation are strigolactone-dependent. *Plant Direct* **2**, e00062.
Ren A., Ahmed R.I., Chen H., Han L., Sun J., Ding A., … Kong Y. (2019) Genome-Wide Identification, Characterization and Expression Patterns of the Pectin Methylesterase Inhibitor Genes in Sorghum bicolor. *Genes* **10**.
Roig-Oliver M., Nadal M., Clemente-Moreno M.J., Bota J. & Flexas J. (2020) Cell wall components regulate photosynthesis and leaf water relations of Vitis vinifera cv. Grenache acclimated to contrasting environmental conditions. *Journal of Plant Physiology* **244**, 153084.
Sannigrahi P., Ragauskas A.J. & Tuskan G.A. (2010) Poplar as a feedstock for biofuels: A review of compositional characteristics. *Biofuels, Bioproducts and Biorefining* **4**, 209–226.
Scheller H.V. (2017) Plant cell wall: Never too much acetate. *Nature Plants* **3**, 17024.
Sechet J., Htwe S., Urbanowicz B., Agyeman A., Feng W., Ishikawa T., … Mortimer J.C. (2018) Suppression of Arabidopsis GGLT1 affects growth by reducing the L-galactose content and

43

borate cross-linking of rhamnogalacturonan-II. *The Plant Journal: for Cell and Molecular Biology* **96**, 1036–1050.
de Souza A., Hull P.A., Gille S. & Pauly M. (2014) Identification and functional characterization of the distinct plant pectin esterases PAE8 and PAE9 and their deletion mutants. *Planta* **240**, 1123–1138.
Su L., Patton E.G., Vilà-Guerau de Arellano J., Guenther A.B., Kaser L., Yuan B., … Mak J.E. (2016) Understanding isoprene photooxidation using observations and modeling over a subtropical forest in the southeastern US. *Atmospheric Chemistry and Physics* **16**, 7725–7741.
Sun Y., Fu R., Dickinson R., Joiner J., Frankenberg C., Gu L., … Fernando N. (2015) Drought onset mechanisms revealed by satellite solar-induced chlorophyll fluorescence: Insights from two contrasting extreme events. *Journal of Geophysical Research: Biogeosciences* **120**, 2427–2440.
Trueba S., Pan R., Scoffoni C., John G.P., Davis S.D. & Sack L. (2019) Thresholds for leaf damage due to dehydration: declines of hydraulic function, stomatal conductance and cellular integrity precede those for photochemistry. *The New Phytologist* **223**, 134–149.
Urbanowicz BR, Peña MJ, Moniz HA, Moremen KW, York WS. Two Arabidopsis proteins synthesize acetylated xylan in vitro. (2014) *The Plant Journal*, **80**, 197-206.
Wei Y, Lin M, Oliver DJ, Schnable PS. (2009) The roles of aldehyde dehydrogenases (ALDHs) in the PDH bypass of Arabidopsis. *BMC Biochemistry* **10**, 1-0.
Willats W.G., McCartney L., Mackie W. & Knox J.P. (2001) Pectin: cell biology and prospects for functional analysis. *Plant Molecular Biology* **47**, 9–27.
Yuan Y., Teng Q., Zhong R., Haghighat M., Richardson E.A. & Ye Z.-H. (2016) Mutations of arabidopsis TBL32 and TBL33 affect xylan acetylation and secondary wall deposition. *Plos One* **11**, e0146460.
Zhong R., Cui D. & Ye Z.-H. (2017) Regiospecific Acetylation of Xylan is Mediated by a Group of DUF231-Containing O-Acetyltransferases. *Plant & Cell Physiology* **58**, 2126–2138.
Zhou J., Zhang Z., Sun G., Fang X., Zha T., McNulty S., … Noormets A. (2013) Response of ecosystem carbon fluxes to drought events in a poplar plantation in Northern China. *Forest Ecology and Management* **300**, 33–42.

44